

Drug-Loaded Carbon Nanohorns: Adsorption and Release of Dexamethasone in Vitro

Tatsuya Murakami,^{†,‡} Kumiko Ajima,[‡] Jin Miyawaki,[‡] Masako Yudasaka,^{‡,§}
Sumio Iijima,^{‡,§,||,⊥} and Kiyotaka Shiba^{*,†,#}

*Department of Protein Engineering, Cancer Institute, Toshima, Tokyo 170-8455, Japan,
SORST/JST, c/o NEC, 34 Miyukigaoka, Tsukuba, Ibaraki 305-8501, Japan, NEC,
34 Miyukigaoka, Tsukuba, Ibaraki 305-8501, Japan, AIST, 1-1-1 Higashi,
Tsukuba, Ibaraki 305-8565, Japan, Department of Material Science and Engineering,
Meijo University, 1-501 Shiogamaguchi, Tempaku, Nagoya 468-8502, Japan, and
CREST/JST, c/o Cancer Institute, Toshima, Tokyo 170-8455, Japan*

Received July 7, 2004

Abstract: Single-wall carbon nanohorns (SWNHs) are recently discovered nanostructured spherical aggregates of graphitic tubes. The unique physicochemical properties of SWNHs, including their large surface area, suggest their possible utility as carriers in drug delivery systems. Here we investigated the in vitro binding and release of the antiinflammatory glucocorticoid dexamethasone (DEX) by as-grown SWNHs and their oxidized form, oxSWNHs. Adsorption analyses using [³H]-DEX determined the amount of DEX adsorbed by oxSWNHs to be 200 mg for each gram of oxSWNHs in 0.5 mg/mL of DEX solution, which was approximately 6 times larger than that obtained for as-grown SWNHs. Adsorption kinetics indicated that oxSWNHs had higher affinity for DEX than as-grown SWNHs. Treatment of oxSWNHs at 1200 °C under H₂, which removed the oxygen-containing functional groups on oxSWNHs, did not diminish the high affinity for DEX, suggesting that oxygen-containing functional groups have little contribution for the affinity. DEX–oxSWNH complexes exhibited sustained release of DEX into phosphate-buffered saline (pH 7.4) at 37 °C and more rapid biphasic release into culture medium. The biological integrity of the released DEX form was confirmed by activation of glucocorticoid response element-driven transcription in mouse bone marrow stromal ST2 cells and induction of alkaline phosphatase in mouse osteoblastic MC3T3-E1 cells. Notably, synthesis of SWNHs does not require a metal catalyst, the toxicity of which could become problematical in clinical use, and no cytotoxicity was observed in cells cultured in the presence of oxSWNHs under our conditions. Taken together, these observations highlight the potential utility of SWNHs in drug delivery systems.

Keywords: Drug delivery systems; carbon nanomaterials; biocompatibility; osteoblast

Introduction

In recent years, biological applications for carbon nanomaterials, including carbon nanotubes (CNTs) and fullerene, have come under close scrutiny.^{1–6} Single-wall carbon nanohorns (SWNHs) are another recently discovered member of the carbon nanomaterial family.⁷ They are aggregates of

graphitic tubes that have closed ends with cone-shaped caps (horns). Each tube has a diameter of 2–3 nm, which is larger than the 1.4 nm of typical single-wall CNTs, while the aggregates are 80–100 nm in diameter and have “dahlia-like” or “bud-like” spherical structures.⁸

* To whom correspondence should be addressed: Department of Protein Engineering, Cancer Institute, Japanese Foundation for Cancer Research, 1-37-1 Kami-Ikebukuro, Toshima, Tokyo 170-8455, Japan. Tel/fax: +81-3-5394-3903. E-mail: kshiba@jfcr.or.jp.

[†] Department of Protein Engineering, Cancer Institute.

[‡] SORST/JST, c/o NEC.

[§] NEC.

^{||} AIST.

[⊥] Meijo University.

[#] CREST/JST, c/o Cancer Institute.

One of the most intriguing features of SWNHs is that they have extensive surface areas and multitudes of horn interstices, which enable large amounts of guest molecules to be adsorbed onto them.⁹ Moreover, the surface area can be further enlarged by oxidization, which causes formation of nanowindows in the SWNH walls.¹⁰ Through these nanowindows, a variety of small molecules [e.g., N₂, Ar, and fullerene (C₆₀)] have been shown to infiltrate into their inner space,¹¹ thus roughly quadrupling the adsorptive surface areas.¹⁰ More interestingly, the sizes of the pores can be controlled by changing the oxidization conditions, and series of oxidized SWNHs (oxSWNHs) having distinct molecular sieving effects can be prepared.^{10,11}

Oxidation also introduces oxygen functional groups (e.g., carboxyl and quinone groups), at the pore edges of ox-SWNHs,¹² which may endow them with yet additional properties. For instance, Kuznetsova et al. reported that the oxygen functional groups sterically regulate the access of

(1) Pantarotto, D.; Partidos, C. D.; Graff, R.; Hoebeke, J.; Briand, J.-P.; Prato, M.; Bianco, A. Synthesis, structural characterization, and immunological properties of carbon nanotubes functionalized with peptides. *J. Am. Chem. Soc.* **2003**, *125*, 6160–6164.

(2) Mattson, M. P.; Haddon, R. C.; Rao, A. M. Molecular functionalization of carbon nanotubes and use as substrate for neuronal growth. *J. Mol. Neurosci.* **2000**, *14*, 175–182.

(3) Chen, R. J.; Bangsaruntip, S.; Drouvalakis, K. A.; Wong Shi Kam, N.; Shim, M.; Li, Y.; Kim, W.; Utz, P. J.; Dai, H. Noncovalent functionalization of carbon nanotubes for highly specific electronic biosensors. *Proc. Natl. Acad. Sci. U.S.A.* **2003**, *100*, 4984–4989.

(4) Pantarotto, D.; Partidos, C. D.; Hoebeke, J.; Brown, F.; Kramer, E.; Briand, J.-P.; Muller, S.; Prato, M.; Bianco, A. Immunization with peptide-functionalized carbon nanotubes enhances virus-specific neutralizing antibody responses. *Chem. Biol.* **2003**, *10*, 961–966.

(5) Park, K. H.; Chhowalla, M.; Iqbal, Z.; Sesti, F. Single-walled carbon nanotubes are a new class of ion channel blockers. *J. Biol. Chem.* **2003**, *278*, 50212–50216.

(6) Pantarotto, D.; Briand, J.-P.; Prato, M.; Bianco, A. Translocation of bioactive peptides across cell membranes by carbon nanotubes. *Chem. Commun.* **2004**, *16*–17.

(7) Iijima, S.; Yudasaka, M.; Yamada, R.; Bandow, S.; Suenaga, K.; Kokai, F.; Takahashi, K. Nano-aggregates of single-walled graphitic carbon nano-horns. *Chem. Phys. Lett.* **1999**, *309*, 165–170.

(8) Kasuya, D.; Yudasaka, M.; Takahashi, K.; Kokai, F.; Iijima, S. Selective production of single-wall carbon nanohorn aggregates and their formation mechanism. *J. Phys. Chem. B* **2002**, *106*, 4947–4951.

(9) Murata, K.; Kaneko, K.; Kanoh, H.; Kasuya, D.; Takahashi, K.; Kokai, F.; Yudasaka, M.; Iijima, S. Adsorption mechanism of supercritical hydrogen in internal and interstitial nanospaces of single-wall carbon nanohorn assembly. *J. Phys. Chem. B* **2002**, *106*, 11132–11138.

(10) Murata, K.; Kaneko, K.; Steele, W. A.; Kokai, F.; Takahashi, K.; Kasuya, D.; Hirahara, K.; Yudasaka, M.; Iijima, S. Molecular potential structures of heat-treated single-wall carbon nanohorn assemblies. *J. Phys. Chem. B* **2001**, *105*, 10210–10216.

(11) Murata, K.; Hirahara, K.; Yudasaka, M.; Iijima, S.; Kasuya, D.; Kaneko, K. Nanowindow-induced molecular sieving effect in a single-wall carbon nanohorn. *J. Phys. Chem. B* **2002**, *106*, 12668–12669.

(12) Bekyarova, E.; Kaneko, K.; Yudasaka, M.; Kasuya, D.; Iijima, S.; Huidobro, A.; Rodriguez-Reinosa, F. Controlled opening of single-wall carbon nanohorns by heat treatment in carbon dioxide. *J. Phys. Chem. B* **2003**, *107*, 4479–4484.

(13) Kuznetsova, A.; Mawhinney, D. B.; Naumenko, V.; Yates, J. T., Jr.; Liu, J.; Smalley, R. E. Enhancement of adsorption inside of single-walled nanotubes: opening the entry ports. *Chem. Phys. Lett.* **2000**, *321*, 292–296.

(14) Hashimoto, A.; Yorimitsu, H.; Ajima, K.; Suenaga, K.; Isobe, H.; Miyawaki, J.; Yudasaka, M.; Iijima, S.; Nakamura, E. Selective deposition of a gadolinium(III) cluster in a hole opening of single-wall carbon nanohorn. *Proc. Natl. Acad. Sci. U.S.A.* **2004**, *101*, 8527–8530.

(15) Shvedova, A. A.; Castranova, V.; Kisin, E. R.; Schwegler-Berry, D.; Murray, A. R.; Gadebsman, V. Z.; Maynard, A.; Baron, P. Exposure to carbon nanotube material: assessment of nanotube cytotoxicity using human keratinocyte cells. *J. Toxicol. Environ. Health A* **2003**, *66*, 1909–1926.

(16) Barroug, A.; Glimcher, M. J. Hydroxyapatite crystals as a local delivery system for cisplatin: adsorption and release of cisplatin in vitro. *J. Orthop. Res.* **2002**, *20*, 274–280.

(17) Chen, J.-F.; Ding, H.-M.; Wang, J.-X.; Shao, L. Preparation and characterization of porous hollow silica nanoparticles for drug delivery application. *Biomaterials* **2004**, *25*, 723–727.

(18) Radin, S.; Ducheyne, P.; Kamplain, T.; Tan, B. H. Silica sol-gel for the controlled release of antibiotics. I. Synthesis, characterization, and in vitro release. *J. Biomed. Mater. Res.* **2001**, *57*, 313–320.

(19) Roy, I.; Ohulchanskyy, T. Y.; Pudavar, H. E.; Bergey, E. J.; Oseroff, A. R.; Morgan, J.; Dougherty, T. J.; Prasad, P. N. Ceramic-based nanoparticles entrapping water-insoluble photosensitizing anticancer drugs: a novel drug–carrier system for photodynamic therapy. *J. Am. Chem. Soc.* **2003**, *125*, 7860–7865.

(20) Lin, F. H.; Lee, Y. H.; Jian, C. H.; Wong, J.-M.; Shieh, M.-J.; Wang, C.-Y. A study of purified montmorillonite intercalated with 5-fluorouracil as drug carrier. *Biomaterials* **2002**, *23*, 1981–1987.

(21) Allen, T. M.; Cullis, P. R. Drug delivery systems: entering the mainstream. *Science* **2004**, *303*, 1818–1822.

(22) Gill, P. S.; Wernz, J.; Scadden, D. T.; Cohen, P.; Mukwaya, G. M.; von Roenn, J. H.; Jacobs, M.; Kempin, S.; Silverberg, I.; Gonzales, G.; Rarick, M. U.; Myers, A. M.; Shepherd, F.; Sawka, C.; Pike, M. C.; Ross, M. E. Randomized phase III trial of liposomal daunorubicin versus doxorubicin, bleomycin, and vincristine in AIDS-related Kaposi's sarcoma. *J. Clin. Oncol.* **1996**, *14*, 2353–2364.

Here we describe our investigation of the ability of SWNHs to bind and release the antiinflammatory glucocorticoid DEX (DEX) *in vitro* and discuss the potential utility of SWNHs as drug carriers.

Experimental Section

Materials. The dahlia-like SWNHs and their oxidized form, oxSWNHs, were prepared as described previously.^{10,26} Briefly, the as-grown SWNHs prepared by laser ablation were oxidized for 10 min in pure oxygen (760 Torr) at 580 °C and then heated at 400 °C for an additional 2 h under ultrahigh vacuum ($\sim 1 \times 10^{-7}$ Torr). The oxSWNHs were further heated at 1200 °C under a H₂ gas flow (760 Torr, 300 cm³ min⁻¹) for 3 h to remove the oxygen-containing functional groups,²⁷ obtaining “oxSWNH-H₂”.

DEX, β -glycerophosphate, ascorbic acid, and FAST *p*-nitrophenyl phosphate tablets were purchased from Sigma (St. Louis, MO). Ethanol (99.5%) was from Wako (Osaka, Japan). [1,2,4-³H]-DEX (1.48 TBq/mmol) was from Amersham Bioscience (Piscataway, NJ). Recombinant human bone morphogenetic protein-4 (rhBMP-4) was from Genzyme/TECHNE (Cambridge, MA). DC Protein Assay kit was from Bio-Rad (Hercules, CA). FuGENE 6 transfection reagent was from Roche Molecular Biochemicals (Mannheim, Germany). Dual-Luciferase Reporter Assay System was from Promega (Madison, WI). Fetal bovine serum (FBS) was from JRH Bioscience (Lenexa, KS). α -Minimum essential medium (α -MEM), RPMI, Dulbecco's phosphate-buffered saline (PBS), and trypsin-EDTA (0.05% trypsin, 0.53 mM EDTA-4Na) were all from Invitrogen (Carlsbad, CA). Penicillin and streptomycin were purchased from Banyu Pharmaceutical Co., LTD (Tokyo, Japan) and Meiji Seika Kaisha, LTD (Tokyo, Japan), respectively. Cell culture dishes were from IWAKI (Tokyo, Japan).

Adsorption of DEX onto oxSWNHs. oxSWNHs (100 μ g/mL) were dispersed by sonication in 0.1–20 mL of a 1:1

- (23) Yokoyama, M.; Okano, T.; Sakurai, Y.; Fukushima, S.; Okamoto, K.; Kataoka, K. Selective delivery of adriamycin to a solid tumor using a polymeric micelle carrier system. *J. Drug Targeting* **1999**, *7*, 171–186.
- (24) Damascelli, B.; Cantu, G.; Mattavelli, F.; Tamplenizza, P.; Bidoli, P.; Leo, E.; Dosio, F.; Cerrotta, A. M.; Di Tolla, G.; Frigerio, L. F.; Garbagnati, F.; Lanocita, R.; Marchiano, A.; Patelli, G.; Spreafico, C.; Ticha, V.; Vespro, V.; Zunino, F. Intraarterial chemotherapy with polyoxyethylated castor oil free paclitaxel, incorporated in albumin nanoparticles (ABI-007): Phase II study of patients with squamous cell carcinoma of the head and neck and anal canal: preliminary evidence of clinical activity. *Cancer* **2001**, *92*, 2592–2602.
- (25) Seiden, M. V.; Muggia, F.; Astrow, A.; Matulonis, U.; Campos, S.; Roche, M.; Silvret, J.; Rusk, J.; Barrett, E. A phase II study of liposomal irinotecan (OSI-211) in patients with topotecan resistant ovarian cancer. *Gynecol. Oncol.* **2004**, *93*, 229–232.
- (26) Ajima, K.; Yudasaka, M.; Suenaga, K.; Kasuya, D.; Azami, T.; Iijima, S. Material storage mechanism in porous nanocarbon. *Adv. Mater.* **2004**, *16*, 397–401.
- (27) Miyawaki, J.; Yudasaka, M.; Iijima, S. Solvent effects on hole-edge structure for single-wall carbon nanotubes and single-wall carbon nanohorns. *J. Phys. Chem. B* **2004**, *108*, 10732–10735.

mixture of ethanol and filtrated (0.22 μ m) H₂O, after which cell culture grade DEX (1000 μ g/mL) in ethanol/H₂O (1:1) solution was added at a volume ratio of 1:1. The resultant mixture was incubated at room temperature overnight and then centrifuged at 18000g for 5 min to collect the DEX–oxSWNH complexes, which were then dried in vacuo overnight for bioassays. The amount of DEX adsorbed onto oxSWNHs was quantified using [³H]-DEX and an LS6500 scintillation counter (Beckman, Fullerton, CA).

Thermogravimetric Analysis (TGA). Thermogravimetric analysis was carried out using a Hi-Res TGA 2950 thermogravimetric analyzer (TA Instruments, New Castle, DE). The temperature was increased from room temperature to 1000 °C at a rate of 10 °C/min under pure O₂ flowing at 100 cm³/min. The gas component evolved at elevated temperatures was sequentially analyzed using a ThermoStar mass spectrometer (Pfeiffer, BUC, France).

In Vitro Release of DEX from DEX–oxSWNHs. DEX–oxSWNHs were prepared as described above by using [³H]-DEX, after which they were incubated at 37 °C in PBS,²⁸ RPMI1640,²⁹ or α -MEM³⁰ supplemented with 5% FBS, 100 μ g/mL penicillin, and 100 units/mL streptomycin. At appropriate times, samples were collected and centrifuged at 18000g for 5 min, and the amount of [³H]-DEX released into the supernatant was quantified using an LS6500 scintillation counter. In the case of cumulative release experiments, the supernatants were replaced with fresh media at each sampling point.

Cell Culture. Mouse bone marrow stromal cell (ST2) and osteoblastic cell (MC3T3-E1) lines were generously provided by Dr. K. Imamura (Cancer Institute, Japanese Foundation for Cancer Research). ST2 and MC3T3-E1 cells were respectively maintained in RPMI1640 and α -MEM supplemented with 10% FBS, 100 μ g/mL penicillin, and 100 units/mL streptomycin in continuous culture at 37 °C under a humidified atmosphere with 5% CO₂ and 95% air. The cells were passaged every 3–4 days.

DEX-Responsive Promoter Assays. An expression vector containing the luciferase reporter gene controlled by DEX-responsive element (pBV2-MMTV-LUC) was the gift by Drs. H. Noguchi and I. Abe of the University of Shizuoka (Shizuoka, Japan).³¹ ST2 cells were seeded to a density of 25000 cells/well in 24-well plates. After incubating for 1 day, they were cotransfected for 5 h with pBV2-MMTV-

- (28) Dulbecco, R.; Vogt, M. Plaque formation and isolation of pure lines with poliomyelitis viruses. *J. Exp. Med.* **1957**, *106*, 167–169.
- (29) Moore, G. E.; Gerner, R. E.; Franklin, H. A. Culture of normal human leukocytes. *JAMA, J. Am. Med. Assoc.* **1967**, *199*, 519–524.
- (30) Stanners, C. P.; Eliceiri, G. L.; Green, H. Two types of ribosome in mouse-hamster hybrid cells. *Nat. New Biol.* **1971**, *230*, 52–54.
- (31) Abe, I.; Umehara, K.; Morita, R.; Nemoto, K.; Degawa, M.; Noguchi, H. Green tea polyphenols as potent enhancers of glucocorticoid-induced mouse mammary tumor virus gene expression. *Biochem. Biophys. Res. Commun.* **2001**, *281*, 122–125.

LUC plus thymidine kinase promoter-driven *Renilla* luciferase DNA (Promega) using FuGENE6, after which the medium was changed to RPMI1640 containing DEX (0, 0.01, 0.05, 0.1, 0.5, or 1.0 μ M), DEX–oxSWNHs (0.01, 0.1, 1, or 10 μ g/mL), or oxSWNHs (0.1, 1, or 10 μ g/mL). After an additional 12 h, luciferase activity was measured using an AutoLumat LB953 (Berthold Technologies, Oak Ridge, TN) and Dual-Luciferase Reporter Assay System according to the manufacturer's instructions.

ALP Assays. MC3T3-E1 cells seeded to a density of 50000 cells/well in 24-well plates were grown until they reached confluence. The culture medium was then changed to a “differentiation-inducing medium”³² consisting of α -MEM supplemented with 5% FBS, 100 units/mL penicillin, 100 μ g/mL streptomycin, 50 μ M ascorbic acid, 10 mM β -glycerophosphate, and 20 ng/mL rhBMP-4 plus DEX (0, 0.01, 0.05, 0.1, 0.5, or 1 μ M), oxSWNHs (2, 10, or 20 μ g/mL), or DEX–oxSWNHs (2, 10, or 20 μ g/mL). The cells were incubated for 10 days, during which the medium was refreshed every 3–4 days. Medium changes were performed carefully so that oxSWNHs or DEX–oxSWNHs adhering to the cells were not washed off and taken with medium.

For ALP assays, the medium was removed and the cells were washed three times with tris-buffered saline [TBS, 20 mM Tris (pH 7.4), 150 mM NaCl], after which they were harvested by scraping them into 250 μ L of TBS containing 0.2% Triton X-100 on ice and then sonicated on ice for 5 min. The resultant cell lysates were centrifuged at 18000g for 10 min at 4 °C, after which aliquots of the supernatant were collected for assay. To assay ALP activity, the supernatant (50 μ L) was mixed with *p*-nitrophosphate according to the manufacturer's protocol, and the amount of *p*-nitrophenol released in 45 min was assessed spectrophotometrically (405 nm) using a model 550 microplate reader (Bio-Rad). In addition, protein in the supernatant was assayed by the Lowry method using a DC Protein Assay kit. ALP activity was then expressed as amount of *p*-nitrophenol released normalized to the total protein concentration.

Results

Nanoextraction for Adsorption of DEX onto oxSWNHs. Yudasaka et al. recently established the conditions by which C_{60} can be introduced into the inner space of CNTs in a liquid phase at ambient temperature.³³ In one of their methods, namely, nanoextraction, C_{60} and CNTs were simply incubated in a solvent that had poor affinity for both C_{60} and CNTs. Because C_{60} molecules are hydrophobic, they assembled within the interior space of the CNTs under these conditions.

We used this approach to load DEX onto oxSWNHs. Whereas the solubility of DEX in organic solvents such as

acetone, ethanol, and chloroform is very high, its solubility in H₂O is only moderate (0.1 mg/mL at 25 °C). We therefore chose a solvent composed of 50% ethanol and 50% H₂O, in which DEX could be dissolved to 1 mg/mL. DEX solution (1 mg/mL) and oxSWNHs suspension (100 μ g/mL) in ethanol/H₂O (1:1) were mixed at a volume ratio of 1:1, and the mixture was incubated overnight, after which the DEX–oxSWNH fraction was collected by centrifugation. As a control, we also prepared an oxSWNH sample that was incubated without DEX. Figure 1A shows TGAs for the DEX–oxSWNHs (black) and oxSWNHs (gray). Differentiation of the curve clearly shows that the weight of the DEX was lost in at least four steps at around 270, 290, 330, and 470 °C (Figure SI 1A, Supporting Information). Corresponding to these peaks, the differential curve for the combustion of DEX–oxSWNHs showed broad peaks at about 290 and 470 °C (Figure SI 1B, Supporting Information).

We also carried out sequential TGA–mass spectrometry measurements using pure DEX (Figure 1B, upper) and DEX–oxSWNHs (Figure 1B, lower). Fluorine (F; *m/z* = 19) evolved from DEX was first detected at about 250 °C, was maximal at about 400 °C, and then gradually declined as the temperature continued to rise (Figure 1B, upper). The gradual decline is usually caused by gradual desorption of fluorine that evolves from specimens but is then adsorbed onto the gas transfer tubes and other parts of the measurement system. Fluorine evolved from DEX–oxSWNHs (Figure 1B, lower) showed a temperature profile similar to that of DEX, confirming that DEX–oxSWNHs does indeed include DEX. The absence of an ion current peak at 400 °C in the case of DEX–oxSWNHs is indicative of the small amount of fluorine actually evolved.

Note that the peak at 210 °C in Figure SI 1B could be due to the decomposition of DEX because TGA–mass spectrometry measurements detected the CO and CO₂ emission (unpublished results). The decomposition of DEX at 210 °C could be catalyzed by the presence of oxSWNHs, which should be confirmed by future experiments.

Kinetics of Adsorption of DEX onto oxSWNHs. The adsorption of DEX onto oxSWNHs was assessed using [³H]-DEX. Preliminary experiments showed that the adsorption plateaus after only a few min of incubation (data not shown). Similarly rapid saturation was also observed for adsorption of cisplatin onto hydroxyapatite crystals.¹⁶ We assumed, therefore, that the binding of DEX to oxSWNHs would reach equilibrium within 1 h and varied the concentration of DEX to monitor the absorption profile. As shown in Figure 2 (squares), the amount of DEX adsorbed onto oxSWNHs increased with increasing concentrations of DEX. The amount of DEX adsorbed by oxSWNHs was determined to be 200 mg for each gram of oxSWNHs in 0.5 mg/mL of DEX solution, which was approximately 6 times larger than that obtained for as-grown SWNHs.

The adsorption profiles indicated that oxSWNHs had higher affinity for DEX than as-grown SWNHs. As described earlier, oxidation of SWNHs introduced the oxygen functional groups at the hole-edges of oxSWNHs.²⁷ To know

(32) Maeda, S.; Hayashi, M.; Komiya, S.; Imamura, T.; Miyazono, K. Endogenous TGF- β signaling suppresses maturation of osteoblastic mesenchymal cells. *EMBO J.* **2004**, 23, 552–563.

(33) Yudasaka, M.; Ajima, K.; Suenaga, K.; Ichihashi, T.; Hashimoto, A.; Iijima, S. Nano-extraction and nano-condensation for C_{60} incorporation into single-wall carbon nanotubes in liquid phases. *Chem. Phys. Lett.* **2003**, 380, 42.

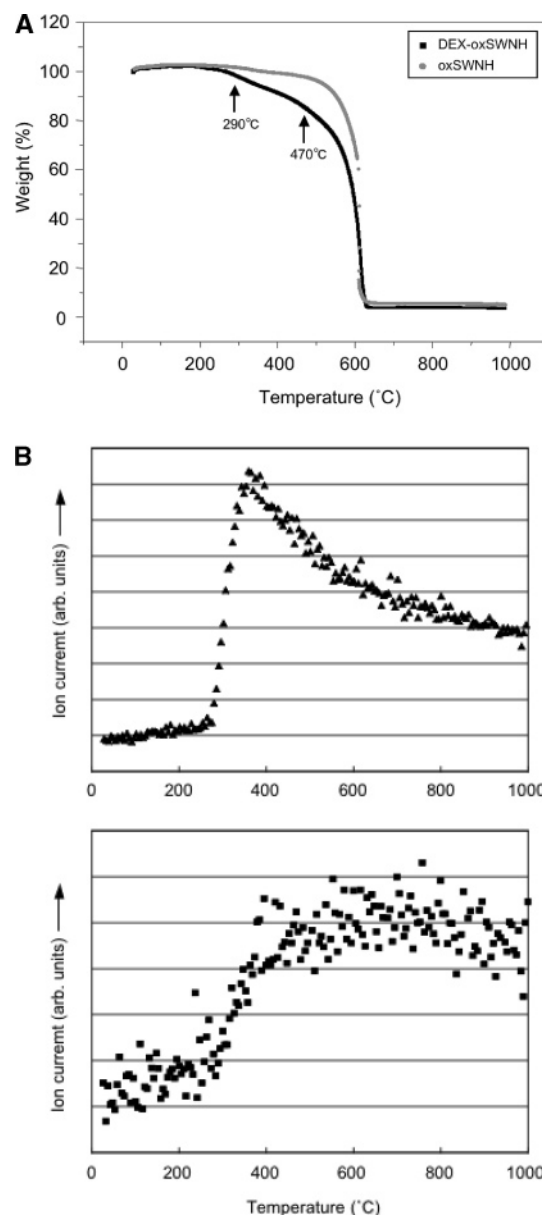


Figure 1. Characterization of DEX–oxSWNHs. (A) Thermo gravimetric analysis (TGA) of DEX–oxSWNHs and oxSWNHs: temperature was increased at 10 °C/min in O₂ flowing at 100 cm³/min; DEX–oxSWNHs (black); oxSWNHs (gray). (B) Thermogravimetric analysis–mass spectrometry profiles at *m/z* = 19 for DEX (upper) and DEX–oxSWNHs (lower). oxSWNHs (100 µg/mL) and DEX (1000 µg/mL) were mixed in ethanol/H₂O (1:1) at a volume ratio of 1:1 and incubated for 1 h. The mixtures were then centrifuged to obtain DEX–oxSWNHs as residues, which were dried in vacuo prior to analysis.

the possible contribution of these oxygen groups in the higher affinity of oxSWNHs for DEX, we removed the groups by heat-treating oxSWNHs in H₂ at 1200 °C for 3 h.²⁷ The resultant oxSWNH-H₂ showed a similar adsorption profile for DEX (Figure 2), indicating that the oxygen-containing groups had little contribution for the higher affinity of oxSWNHs.

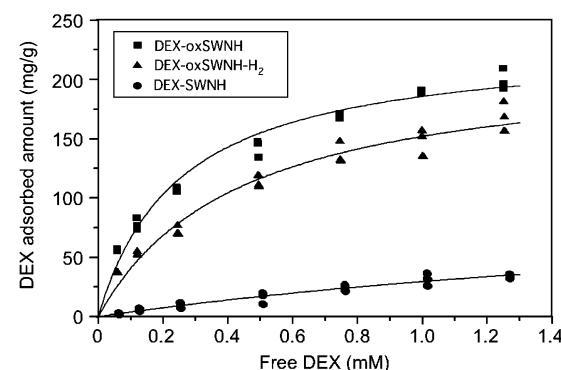


Figure 2. Langmuir adsorption isotherms describing adsorption of DEX by oxSWNHs, oxSWNH-H₂s, and SWNHs in a 1:1 ethanol/H₂O mixture: plotted is the amount of DEX adsorbed vs the steady-state drug concentration; DEX–oxSWNHs (closed squares); DEX–oxSWNH-H₂s (closed triangles); DEX–SWNHs (closed circles). oxSWNHs, oxSWNH-H₂s, or SWNHs (50 µg/mL) and the indicated concentrations of DEX containing [³H]-DEX were mixed in 1:1 ethanol/H₂O and incubated overnight. The mixtures were then centrifuged and DEX–oxSWNHs, DEX–oxSWNH-H₂s, or SWNHs in the residues were quantified using a liquid scintillation counter.

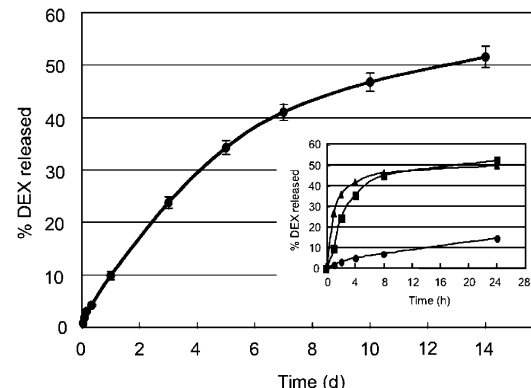


Figure 3. Time course of the cumulative release of DEX from DEX–oxSWNHs in PBS. DEX–oxSWNHs prepared with [³H]-DEX were dispersed in PBS at 0.005 wt % and incubated at 37 °C. At the indicated times, the PBS was refreshed, and the DEX released into the collected PBS was measured using a liquid scintillation counter. Total amounts of DEX released up to the indicated times were expressed as percentages of the total DEX bound to DEX–oxSWNHs. The inset shows cumulative release of DEX from DEX–oxSWNHs in PBS (closed circles), RPMI1640 (closed squares), and α-MEM/5% FBS (closed triangles) at 37 °C.

In Vitro Release of DEX from DEX–oxSWNHs. Controlled release of drugs from a drug–carrier complex is required as a cardinal property of drug delivery systems.²¹ Figure 3 illustrates the cumulative dose of DEX released from DEX–oxSWNHs in PBS (pH 7.4) at 37 °C. During the first few days, the amount of DEX released was nearly proportional to the incubation time, i.e., 7–10% per day. The release rate then gradually declined, and about 50% of the total bound DEX was released from the complex within a period of 2 weeks.

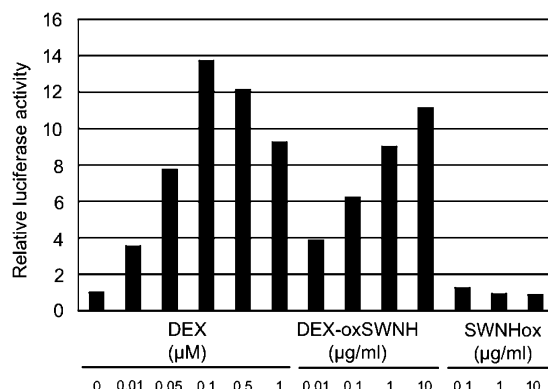


Figure 4. Effects of DEX-oxSWNHs and oxSWNHs on GR transcriptional activity. ST2 cells were transfected with pBV2-MMTV-LUC and treated with DEX, DEX-oxSWNHs, or oxSWNHs for 12 h. Firefly luciferase activity was measured in the cells lysates and normalized to the *Renilla* luciferase activity. The values in the figure represent the means of duplicate determinations.

When cell culture medium was used instead of PBS, distinctly different release profiles were obtained (Figure 3, inset). Almost half of the DEX was released within the first 8 h, after which the release rates sharply declined, so that by 24 h about 50% of the total bound DEX had been released into the RPMI1640. As mentioned above, only about 10% was released into PBS during the same time period. One possible explanation for this difference in the release profiles is that hydrophobic organic compounds present in the culture medium are competitively absorbed onto the surface of oxSWNHs, or they may increase the apparent solubility of DEX in medium.

Biological Activity of DEX Released from DEX-oxSWNHs. DEX is a synthetic glucocorticoid receptor (GR) agonist. A member of the nuclear receptor family, GR binds to glucocorticoid response elements (GREs) and activates transcription in a glucocorticoid-dependent manner.³⁴ We examined the responsiveness of GREs to DEX released from DEX-oxSWNHs using a reporter plasmid, pBV2-MMTV-LUC, which contains a luciferase gene under the control of GREs.³¹ For this purpose, we first transfected ST2 cells³⁵ with pBV2-MMTV-LUC, after which the cells were incubated with increasing amounts of DEX-oxSWNHs, free DEX, or oxSWNHs. As shown in Figure 4, free DEX (0.01–0.1 μM) activated expression of luciferase in a concentration-dependent manner. In addition, for reasons we do not understand, at concentrations >0.1 μM free DEX concentration-dependently suppressed activation of luciferase to levels below that seen at 0.1 μM. Treatment of the transfected cells with DEX-oxSWNHs for 12 h also dose-dependently

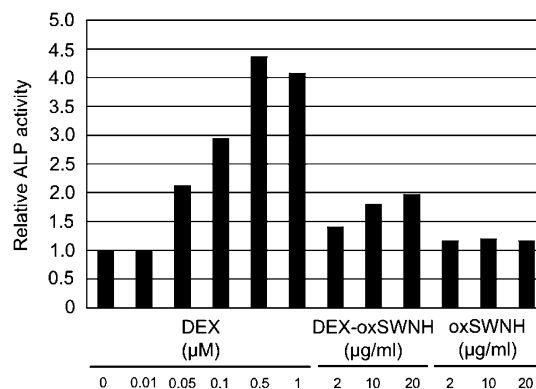


Figure 5. Effects of DEX-oxSWNHs and oxSWNHs on ALP activity. MC3T3-E1 cells were cultured for 10 days in α-MEM containing 5% FBS, 50 μM ascorbic acid, 10 mM β-glycero-phosphate, and 20 ng/mL rhBMP-4 plus DEX (0.01, 0.05, 0.1, 0.5, 1 μM) or oxSWNHs or DEX-oxSWNHs (2, 10, 20 μg/ml). The media were changed every 3–4 days without addition of oxSWNHs or DEX-oxSWNHs. ALP activity was measured using *p*-nitrophenyl phosphate as a substrate and normalized to the protein concentration. Relative ALP activity is shown as 0–5-fold induction. The values in the figure represent the means of duplicate determinations.

activated luciferase expression, whereas empty oxSWNHs induced no activation.

DEX is also known to promote differentiation of pre-osteoblasts into mature osteoblasts, and expression of ALP is often used as a marker of that differentiation.³⁶ As such, preosteoblastic MC3T3-E1 cells reportedly exhibit increased expression of ALP following treatment with DEX plus bone morphogenetic protein (BMP)-2, which is a potent promoter of osteoblast differentiation and bone formation.^{37–39} We confirmed that treating MC3T3-E1 with DEX-oxSWNHs in the presence of BMP-2 also increased expression of ALP. As shown in Figure 5, the addition of DEX-oxSWNHs to MC3T3-E1 cell cultures dose-dependently increased ALP activity, whereas empty oxSWNHs had no effect.

Taken together, the results of the two *in vitro* cell assays described above indicate that the DEX released from DEX-

(34) Yamamoto, K. R. Steroid receptor regulated transcription of specific genes and gene networks. *Annu. Rev. Genet.* **1985**, *19*, 209–252.
 (35) Rubin, J.; Biskobing, D. M.; Jadhav, L.; Fan, D.; Nanes, M. S.; Perkins, S.; Fan, X. Dexamethasone promotes expression of membrane-bound macrophage colony-stimulating factor in murine osteoblast-like cells. *Endocrinology* **1998**, *139*, 1006–1012.

(36) Diefenderfer, D. L.; Osyczka, A. M.; Garino, J. P.; Leboy, P. S. Regulation of BMP-induced transcription in cultured human bone marrow stromal cells. *J. Bone Surg. Am.* **2003**, *85-A Suppl. 3*, 19–28.
 (37) Luppen, C. A.; Smith, E.; Spevak, L.; Boskey, A. L.; Frenkel, B. Bone morphogenetic protein-2 restores mineralization in glucocorticoid-inhibited MC3T3-E1 osteoblast cultures. *J. Bone Miner. Res.* **2003**, *18*, 1186–1197.
 (38) Luppen, C. A.; Leclerc, N.; Noh, T.; Barski, A.; Khokhar, A.; Boskey, A. L.; Smith, E.; Frenkel, B. Brief bone morphogenetic protein 2 treatment of glucocorticoid-inhibited MC3T3-E1 osteoblasts rescues commitment-associated cell cycle and mineralization without alteration of Runx2. *J. Biol. Chem.* **2003**, *278*, 44995–45003.
 (39) Shui, C.; Scutt, A. M. Mouse embryo-derived NIH3T3 fibroblasts adopt an osteoblast-like phenotype when treated with 1α,25-dihydroxyvitamin D₃ and dexamethasone *in vitro*. *J. Cell Physiol.* **2002**, *193*, 164–172.

oxSWNHs is indeed biologically active. To our knowledge, this is the first time either SWNHs or CNTs have been evaluated for their utility as drug carriers with mammalian cells.

Discussion

In the present study, we investigated the adsorption of DEX onto the oxidized form of single-wall carbon nanohorns (oxSWNHs) and its subsequent release in vitro. By incubating DEX and oxSWNHs in a poor solvent for them (1:1 H₂O/ethanol), 200 mg/g DEX was loaded onto oxSWNHs, which was 6 times larger for as-grown SWNHs. Adsorption profiles indicated that oxSWNHs had higher affinity for DEX than as-grown SWNHs. It is known that oxidation introduces various oxygen functional groups (e.g., carboxyl, carbonyl, and hydroxyl groups) onto the external surfaces of graphite sheets of SWNHs and CNTs.^{12,13} We thought at first that these functional groups were likely responsible for the higher affinity of DEX for oxSWNHs. However, the H₂-treatment of oxSWNHs, which has been shown to reduce the oxygen functional groups of oxSWNHs,²⁷ did not diminish the affinity for DEX, concluding little contributing of oxygen functional groups for the increased affinity.

The oxidized SWNHs have nanowindows in their walls,¹⁰ through which small molecules can infiltrate into the inner space of SWNHs.⁹ It has been already shown that the interior surfaces of SWNHs had a stronger binding energy for H₂ and N₂,^{9,10} suggesting the possible contribution of the interior surfaces of the oxSWNHs for the increased affinity for DEX.

DEX–oxSWNHs slowly released DEX into PBS (Figure 3). Kallinteri et al. reported that DEX-liposomes released 25–50% of their DEX into tris-buffered saline (pH 7.4) over 48 h at 37 °C.⁴⁰ Although the rate of DEX release from DEX–oxSWNHs is comparable, the mechanisms underlying the slow release rates in these two systems differ. In liposomes, a well-established drug carrier system, vesicle stability is a critical determinant of release rate, whereas the rate of dissociation of DEX from the surface of oxSWNHs is the key determinant in the present case.

The release profiles differed substantially when DEX–oxSWNHs were incubated in cell culture medium instead of PBS (Figure 3, inset): at least two release phases, fast and slow, were observed. This suggests that there are at least two modes of interaction between DEX and oxSWNHs, which remain to be characterized.

DEX–oxSWNHs activated GR-mediated transcription (Figure 4). The activation obtained with 0.1 μg/mL DEX–oxSWNHs was comparable with that obtained with 0.01–0.05 μM free DEX. DEX–oxSWNHs contained approximately 200 mg/g DEX (Figure 1), so that 0.1 μg/mL of DEX–oxSWNHs would be expected to release enough DEX to reach a concentration of 0.051 μM. Moreover, given the biphasic kinetics of its release into RPMI1640 (Figure 3,

inset), we would further expect approximately 25% of the total bound DEX to be released within the first 2 h, with about 50% being released within 24 h. This expectation was confirmed in a separate experiment in which DEX was released from 0.1 μg/mL [³H]-DEX–oxSWNHs to a concentration of 0.018 μM (35% of the total bound) in RPMI1640 within 12 h (data not shown). These results explain well how corresponding levels of activation were obtained with 0.1 μg/mL DEX–oxSWNHs and 0.01–0.05 μM free DEX.

As compared with the GR-mediated transcriptional activation, the ALP activity induced by DEX–oxSWNHs was relatively moderate (Figure 5). This may be because the culture medium was refreshed twice (on days 3 and 6) during the ALP experiments without adding new DEX–oxSWNHs. Since approximately half of the DEX bound to DEX–oxSWNHs was released into the culture medium within the first 24 h (Figure 3, inset), MC3T3-E1 cells were probably not exposed to an effective concentration of DEX after the first medium change on day 3. It is noteworthy that we did not observe any adverse effects of DEX–oxSWNHs on cell growth or differentiation, which is in contrast to the reported toxicity of CNT.¹⁵

In summary, we have demonstrated that DEX–oxSWNHs are attractive candidates for use in a novel drug delivery system. DEX–oxSWNHs exhibited sustained release of biologically active DEX in mammalian cells without significant side effects. At present, we are working on direct observation of drugs in oxSWNHs and on in vivo analyses.

Abbreviations Used

ALP, alkaline phosphatase; BMP-2, bone morphogenetic protein-2; C₆₀, fullerene; CNT, carbon nanotube; DEX, dexamethasone; EDTA, ethylenediaminetetraacetic acid; FBS, fetal bovine serum; GR, glucocorticoid receptor; GRE, glucocorticoid response element; MS, mass spectrometry; ox-SWNH, oxidized SWNH; oxSWNH-H₂, H₂-treated oxSWNH; oxSWNT, oxidized SWNT; PBS, phosphate-buffered saline; BMP-2, bone morphogenetic protein-2; SWNH, single-wall carbon nanohorn; SWNT, single-wall carbon nanotube; TBS, tris-buffered saline; TGA, thermogravimetric analysis.

Acknowledgment. The authors thank Dr. S. Utsumi for determining the surface area of oxSWNHs using N₂ adsorption isotherms. The authors also gratefully acknowledge gifts of MC3T3-E1 and ST2 cells from Dr. K. Imamura at the Cancer Institute, Japanese Foundation for Cancer Research, and pBV2-MMTV-LUC from Drs. H. Noguchi and I. Abe at the University of Shizuoka.

Supporting Information Available: Figure depicting derivatives of weight–temperature profiles (TG curves) measured under the same conditions shown in Figure 1 for DEX and DEX–oxSWNHs. This material is available free of charge via the Internet at <http://pubs.acs.org>.

(40) Kallinteri, P.; Antimisiaris, S. G.; Karnabatidis, D.; Kalogeropoulos, C.; Tsota, I.; Siablis, D. Dexamethasone incorporating liposomes: an in vitro study of their applicability as a slow releasing delivery system of dexamethasone from covered metallic stents. *Biomaterials* **2002**, *23*, 4819–4826.